Synthesis, Characterization, and Properties of Novel Organic/Inorganic Epoxy Hybrids Containing Nitrogen/Silicon via the Sol–Gel Method

Ri-Cheng Chang,[1] Chin-Lung Chiang,[1] Yie-Chan Chiu[2]

[1]*Department of Industrial Safety and Health, Hung-Kuang University, Sha-Lu, Taiwan 433, Republic of China*
[2]*Department of Chemical Engineering, National Tsing-Hua University, Hsin-Chu, Taiwan 30043, Republic of China*

Received 8 September 2006; accepted 30 March 2007
DOI 10.1002/app.26994
Published online 17 August 2007 in Wiley InterScience (www.interscience.wiley.com).

ABSTRACT: Organic–inorganic hybrids were prepared with a diglycidyl ether of bisphenol A (DGEBA) type epoxy and silane-modified isocyanuric acid triglycidyl ester via the sol–gel process. The DGEBA-type epoxy was modified by a coupling agent to improve the compatibility of the organic and inorganic phases. The sol–gel technique was used successfully to incorporate silicon and nitrogen into the network of hybrids, increasing the thermal stability. Fourier transform infrared and ^{29}Si-NMR were used to characterize the structures of the hybrids. The results revealed that trisubstituted siloxane bonds (T^3) was the major environment forming a network structure. The morphology of the ceramer was examined with scanning electron microscopy, Si mapping, and transmission electron microscopy. The particle sizes were less than 100 nm. The hybrids were nanocomposites. The ultraviolet–visible spectra of the epoxy hybrid showed no obvious absorbance over a range of 400–800 nm. This phenomenon revealed that the hybrids were transparent. The thermogravimetric analysis revealed that the char yields of the hybrids increased with the contents of the inorganic components. The integral procedure decomposition temperatures of the hybrids were higher than that of the pure epoxy. The thermal stability of the hybrids increased with the contents of the inorganic components. The inorganic components could improve the thermal stability of the pure epoxy. © 2007 Wiley Periodicals, Inc. J Appl Polym Sci 106: 3290–3297, 2007

Key words: composites; silicones; synthesis; thermal properties; thermogravimetric analysis

INTRODUCTION

Epoxy resins have been commercially available for about 50 years and are widely used in modern industries. Research efforts to improve the properties of epoxy resins, including their thermal stability, are in progress to meet the requirements of versatile and advanced applications. The formation of stable char is one of the desirable mechanisms of flame retardation in polymers because the char layer acts both as a thermal insulator and as a barrier to oxygen diffusion. A good way of enhancing char formation is the addition of inorganic fillers because the presence of the inherently stable inorganic phase makes the char mechanically stronger, consequently improving its insulating and barrier properties. In recent times, nanocomposites have emerged as a promising class of materials with good fire retardance.[1–3]

Organic–inorganic hybrid materials are nanophase-separated metal oxide clusters connected to a continuous polymer network via a coupling agent.[4,5] These materials have drawn considerable attention in recent years because of improvements in various properties, including the thermal stability, flame retardancy, and mechanical properties.[6–9]

An interesting method for obtaining these hybrids is the *in situ* sol–gel process, which allows silica domains to be added into the polymer network. It involves a series of hydrolysis and condensation reactions starting from a hydrolyzable, multifunctional alkoxysilane as a precursor for the inorganic domain formation. The advantage of the sol–gel process over the traditional ceramic synthesis process is the ability to form pure and homogeneous products at a low temperature.[10] The use of a suitable coupling agent permits an interconnected network to be obtained, which prevents macroscopic phase separation. The coupling agent provides covalent bonding between the organic and inorganic phases; therefore, well-dispersed nanostructured phases may result.[11]

In this study, novel organic/inorganic epoxy hybrids containing nitrogen/silicon were prepared via the sol–gel method. The structures of the monomers and hybrids were characterized with Fourier

Correspondence to: C.-L. Chiang (dragon@sunrise.hk.edu.tw).

Contract grant sponsor: National Science Council of the Republic of China; contract grant number: NSC 94-2622-E-241-002-CC3.

transform infrared (FTIR), ^{1}H-NMR, and ^{29}Si-NMR. The thermal and morphological properties were examined with thermogravimetric analysis (TGA), differential scanning calorimetry (DSC), scanning electron microscopy (SEM), and transmission electron microscopy (TEM).

EXPERIMENTAL

Materials

The epoxy resin was diglycidyl ether of bisphenol A (DGEBA; NPEL-128), which was generously provided by Nan Ya Plastics Corp. (Taipei, Taiwan). 3-Isocyanatopropyltriethoxysilane (IPTS) was purchased from United Chemical Technologies, Inc. (Bristol, PA). Isocyanuric acid triglycidyl ester (IATE) was obtained from Tokyo Chemical Industry Co., Ltd. (Tokyo, Japan). 3-Aminopropyltriethoxysilane (APTS) was supplied by Acros Organics Co. (3A2440 Geel, Janssens Pharmaceuticalaan, Belgium). Poly(oxypropylene) diamine (Jeffamine D400) was from Huntsman Corp. (Salt Lake City, UT). *N*,*N*-Dimethylacetamide (DMAc) was from Tedia Co. (Farfield, OH). Tetrahydrofuran (THF) was reagent-grade and was supplied by Echo Chemical Co., Ltd. (Hsinchu, Taiwan). Concentrated hydrochloric acid was obtained from Union Chemical Works, Ltd. (Hsinchu, Taiwan). Isopropyl alcohol was purchased from Tedia.

Preparation of the IPTS–epoxy/silane-modified isocyanuric acid triglycidyl ester (SM-IATE) hybrid materials

The hybrid ceramers were prepared through the mixture of two solutions, A and B. Solution A consisted of the modified epoxy resin and THF as a solvent. The modified epoxy resin was synthesized as follows: 4 g of IPTS (equivalent weight = 247 g) was added to 10 g of the DGEBA-type epoxy resin (equivalent weight = 180 g) at 60°C, and the mixture was then stirred for 4 h until the characteristic peak of the NCO group disappeared. IPTS reacted with epoxy to form IPTS–epoxy.[12] Solution B was composed of IATE and APTS in a molar ratio of 3:1. IATE was dissolved in DMAc, and its solid content was 20 wt %. APTS was then slowly poured into the IATE solution and mixed at 50°C for 12 h. APTS was incorporated into IATE to form SM-IATE. HCl was used as the catalyst for hydrolysis. D400 was used as the curing agent of the modified epoxy resin. The IPTS–epoxy/SM-IATE hybrid materials were prepared with various SM-IATE feed ratios (Table I). The mixtures were stirred until the solutions became clear. The solutions were cast into aluminum dishes to gel at room temperature. The wet gels were aged at room temperature for 48 h and were then dried at 80°C for 2 h in a vacuum oven. The samples were placed in a vacuum oven at 150°C for 4 h and then cured at 160°C for 24 h.

Reaction schemes

The novel hybrid materials were prepared as described in Schemes 1–3.

FTIR spectroscopy

To identify the functional groups of the monomers and nanocomposites, FTIR spectra were recorded between 4000 and 400 cm^{-1} with a resolution of 2 cm^{-1} on a Nicolet (United States) Avatar 320 FTIR spectrometer and then scanned more than 32 times. Thin films were prepared by the solution-casting method for the monomer. The films were prepared through the mixing of finely ground solid samples with powered potassium bromide, and the mixtures were pressed under high pressure at 8000–10,000 kg/cm^2.

Solid state ^{29}Si-NMR spectroscopy

^{29}Si-NMR was performed with a Bruker (Rheinstetten, Germany) DSX-400WB. The samples were treated at 180°C for 2 h and then ground into a fine powder.

TGA

The thermal degradation of the hybrids was investigated with a PerkinElmer TGA 7 thermogravimetric analyzer from room temperature to 800°C under a nitrogen atmosphere. The measurements were conducted with 6–10-mg samples. The weight-loss/temperature curves were recorded.

DSC

The glass-transition temperatures (T_g's) of the samples were measured with a DuPont model 10 differential scanning calorimeter. The heating rate was

TABLE I
Compositions of the Epoxy/SM-IATE Hybrid Materials

Sample	Epoxy (wt %)	SM-IATE (wt %)	N (wt %)	Si (wt %)	N + Si (wt %)
Epoxy	100	0	0.00	0.00	0.00
SM-IATE 5	95	5	3.26	2.05	5.31
SM-IATE 10	90	10	3.55	2.40	5.95
SM-IATE 15	85	15	3.84	2.75	6.59

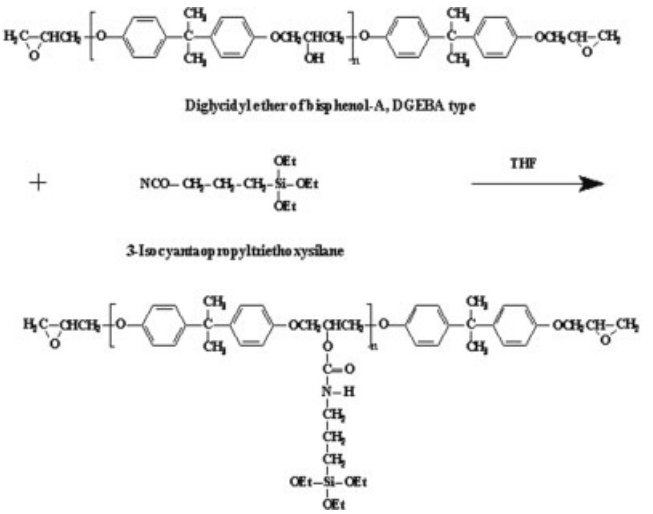

Scheme 1 Reaction process and structure of IPTS–epoxy.

10°C/min within a temperature range of 50–200°C. The measurements were made with 3–4-mg samples on a DSC plate after the specimens were quickly cooled to room temperature after the first scan. T_g's were determined as the midpoint of the transition point of the heat capacity change, and the reproducibility of the T_g values was estimated to be within 2°C.

Morphological properties

The morphology of the fractured surfaces of the nanocomposites was observed with a scanning electron microscope (JSM 840A, JEOL, Tokyo, Japan).

Si mapping technology

Energy-dispersive X-ray (EDX) measurements were conducted with SEM EDX mapping (JSM 840A, JEOL). The white points in the figures denote Si atoms.

TEM

The TEM study was carried out with a Hitachi (Tokyo, Japan) H-7500 with a measured acceleration voltage of 100 kV. The samples were microtomed with a Leica Ultracut (Wetzlar, Germany) into 60-nm-thick slices. These slices were placed on 200-mesh copper nets for TEM observation.

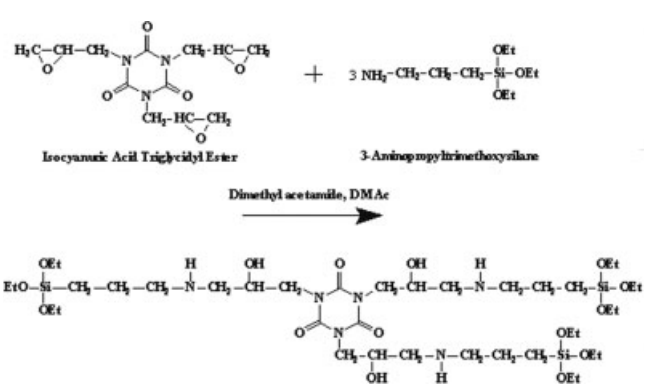

Scheme 2 Reaction process and structure of SM-IATE.

Ultraviolet–visible (UV–vis) spectra

UV–vis spectra were tested on a Hitachi U-3300 spectrophotometer, and the samples were prepared as thin films on a glass substrate by spin coating.

Dynamic mechanical analysis

The dynamic mechanical tests were carried out on a dynamic mechanical thermal analyzer (DMTA MK III, Polymer Laboratory, Oratories, UK) between 30 and 200°C with a heating rate 2°C/min at a frequency of 2 Hz. The rectangular bending mode was chosen, and the dimensions of the specimens were $40 \times 7 \times 3$ mm^3.

RESULTS AND DISCUSSION

Characterization

FTIR of the reaction

The study of the reaction between the epoxy and IPTS in Scheme 1 was reported in our previous arti-

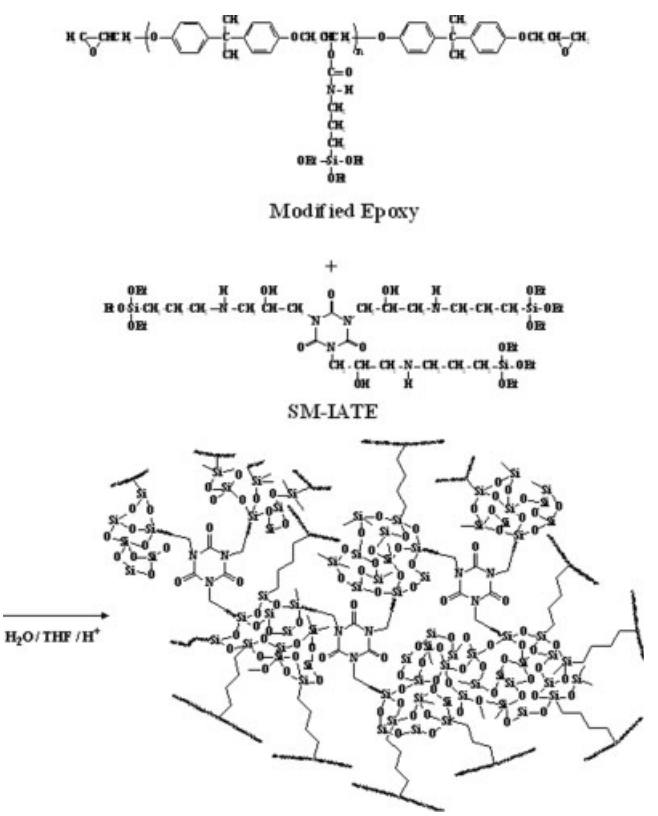

Scheme 3 Reaction process and structure of the epoxy/SM-IATE hybrid.

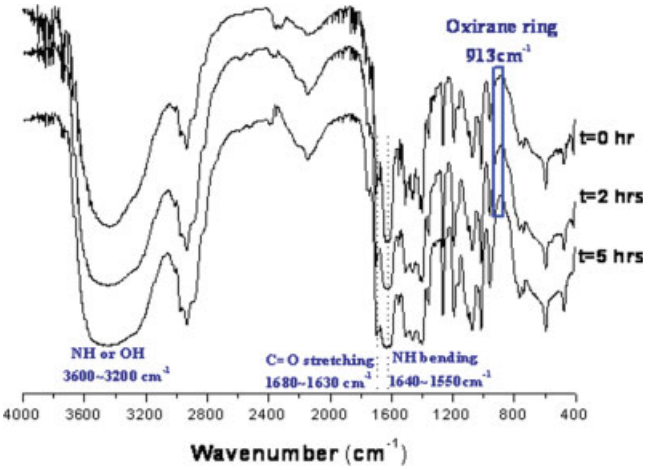

Figure 1 FTIR spectra of the reaction between IATE and APTS. [Color figure can be viewed in the online issue, which is available at www.interscience.wiley.com.]

cle.[12] After the reaction, the epoxy resin possesses the functional group of —OEt to advance the sol–gel reaction. This can enhance the miscibility between the organic and inorganic components.

The chemical structure of SM-IATE was characterized with FTIR and NMR. In this study, we used the amino group of APTS to react with the oxirane group of IATE. The reaction process and structure of SM-IATE are shown in Scheme 2. Figure 1 shows FTIR spectra of the reaction between IATE and APTS. Figure 2 presents FTIR spectra of the oxirane group during the reaction between IATE and APTS. After the reaction, the consumption of the oxirane group and the formation of the secondary—OH group were observed by the disappearance of the absorption at 913 cm^{-1} and the appearance of the absorption between 3600 and 3000 cm^{-1}, respectively.

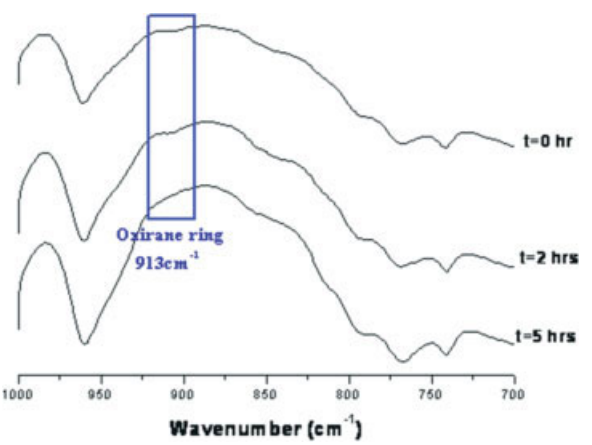

Figure 2 FTIR spectra of the reaction between IATE and APTS. [Color figure can be viewed in the online issue, which is available at www.interscience.wiley.com.]

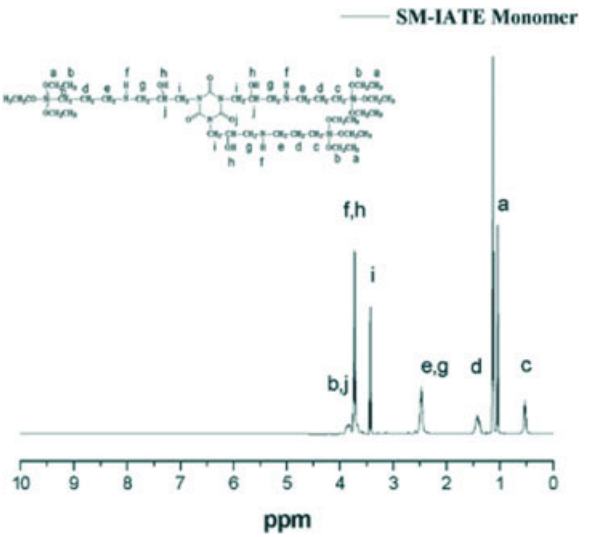

Figure 3 ^{1}H-NMR spectrum of the SM-IATE monomer. [Color figure can be viewed in the online issue, which is available at www.interscience.wiley.com.]

^{1}H-NMR of the monomer

Figure 3 presents the ^{1}H-NMR spectrum of SM-IATE with characteristic shifts of hydrogen at δ = 3.52 (—OH, which is from the opening ring of oxirane), δ = 3.77 (—Si—O—CH_2CH_3), and δ = 1.19 (—Si—O—CH_2CH_3). All these characteristic NMR bands indeed match the expected SM-IATE structure. Other characteristic shifts are as follows: 3.61 (H, $NCH_2CHOHCH_2NH$), 3.52 (H, $NCH_2CHOHCH_2NH$), 3.52 (H, $NCH_2CHOHCH_2NH$), 3.4 (2H, $NCH_2CHOHCH_2NH$), 2.4 (2H, $NHCH_2CH_2CH_2Si$), 2.48 (2H, $NCH_2CHOH\ CH_2NH$), 1.47 (2H, $NHCH_2CH_2CH_2Si$), 1.19 (3H, $SiOCH_2CH_3$), and 0.34 ppm (2H, $NHCH_2CH_2CH_2Si$).

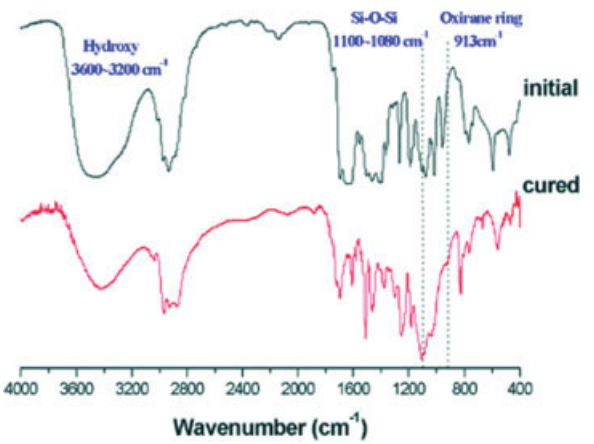

Figure 4 FTIR spectra of the epoxy/SM-IATE hybrid. [Color figure can be viewed in the online issue, which is available at www.interscience.wiley.com.]

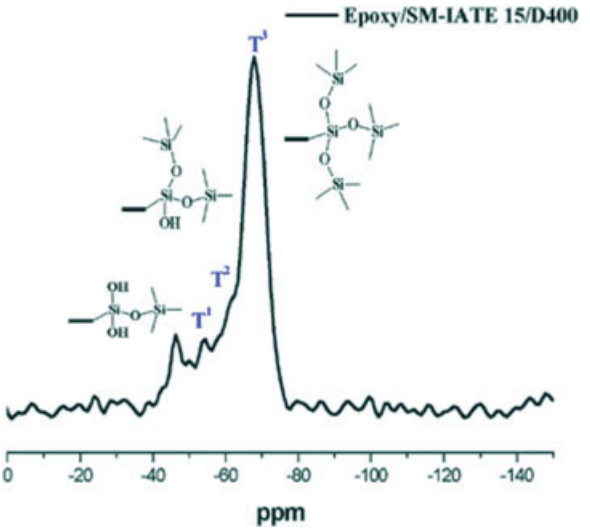

Figure 5 Solid-state ^{29}Si-NMR spectra of epoxy/SM-IATE 15. [Color figure can be viewed in the online issue, which is available at www.interscience.wiley.com.]

FTIR of the hybrid

Infrared spectroscopy was used to characterize the formation of an inorganic backbone through the sol–gel reactions. Scheme 3 shows the reaction process and structure of the epoxy/SM-IATE hybrid. Figure 4 shows FTIR spectra of the epoxy/SM-IATE hybrid. The Si—O—Si group can be detected in the hybrid at 1100–1080 cm^{-1}. This indicates that the condensation reaction of Si—OH happened. It formed the connections between the organic and inorganic phases. There were covalent bonds between the organic and inorganic moieties. The peak at 913 cm^{-1} disappeared in the cured hybrid. This implied that the oxirane rings reacted with the curing agent completely. The hybrids possessed the networks, which enhanced the thermal properties.

^{29}Si-NMR of the hybrid

Figure 5 shows solid-state ^{29}Si-NMR spectra of epoxy/SM-IATE. For IPTS, the monosubstituted, disubstituted, and trisubstituted siloxane bonds are designated T^1, T^2, and T^3, respectively. T^s can be defined as follows:

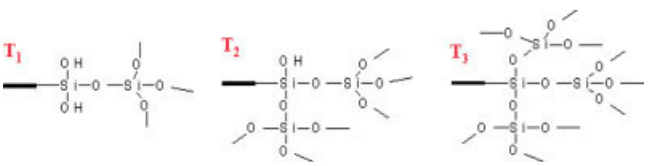

The chemical shifts of T^2 and T^3 are −56 and −65 ppm, respectively, and conform to the literature values.[13] The results reveal that the T^3 bonds were the major microstructures forming the network structure. The network structure promoted the thermal stability of the epoxy resin.

Morphological properties

Figure 6 presents an SEM photograph of the morphology of the composites. Figure 7 shows Si mapping of the epoxy nanocomposites. The fracture surface was very dense. According to these figures, the particles were uniformly dispersed in the polymer matrix

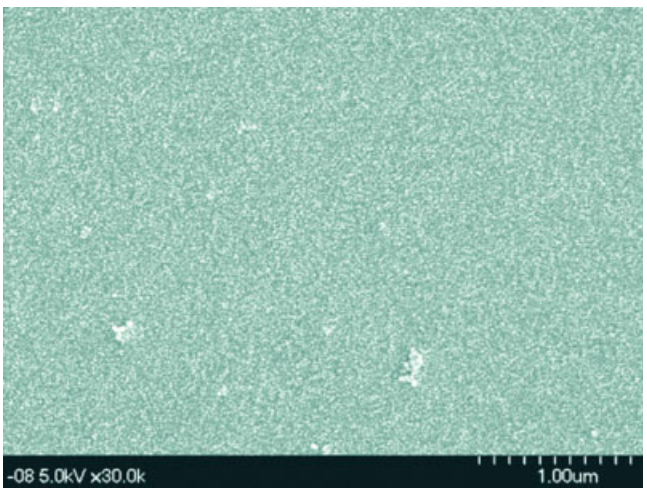

Figure 6 SEM microphotograph of the fractured surface of epoxy/SM-IATE 15. [Color figure can be viewed in the online issue, which is available at www.interscience.wiley.com.]

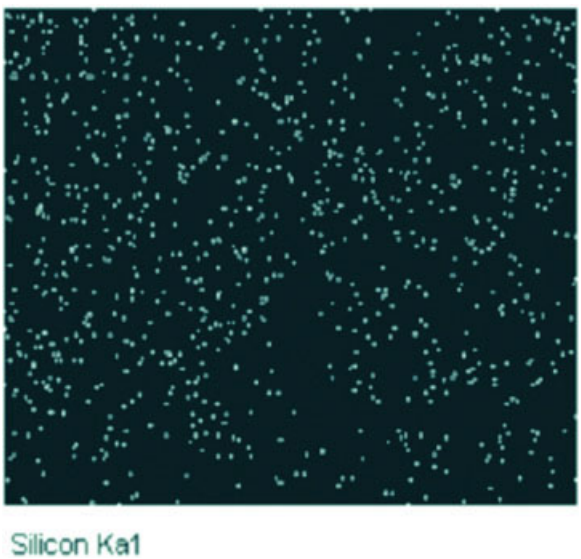

Figure 7 Si mapping of the epoxy/SM-IATE 15 fractured surface. [Color figure can be viewed in the online issue, which is available at www.interscience.wiley.com.]

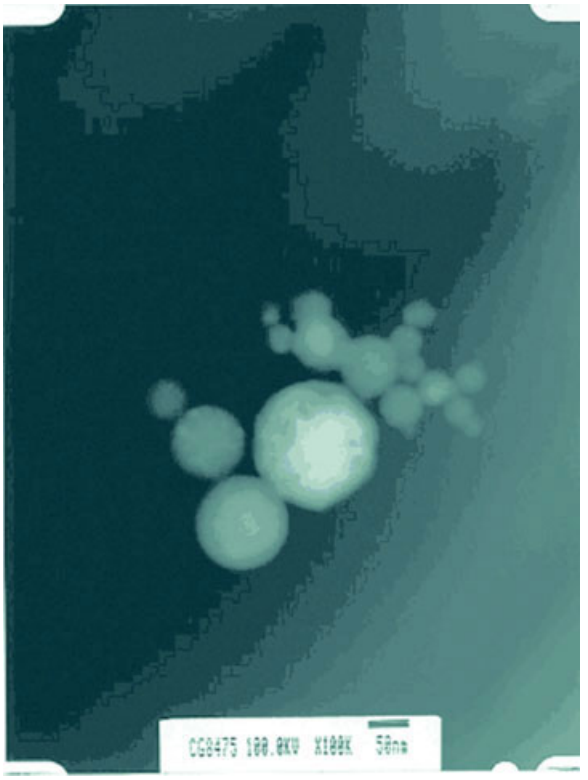

Figure 8 TEM microphotograph of the fractured surface of epoxy/SM-IATE 15/D400. [Color figure can be viewed in the online issue, which is available at www.interscience.wiley.com.]

without macrophase separation. Separated epoxy and inorganic components domains were not observed, and this demonstrated the homogeneity. This result revealed that the nanocomposites exhibited good compatibility between the organic and inorganic phases. Figure 8 presents a TEM microphotograph of the fractured surface of epoxy/SM-IATE 15. According to this figure, the particles were less than 100 nm in size. The hybrids were nanocomposites. Figure 9 shows a photograph of the epoxy/SM-IATE 15 hybrid, which possessed good transparency. Figure 9 shows that the epoxy/SM-IATE 15 hybrid had a clear appearance and a little yellow color. The results give sufficient support for the formation of an epoxy hybrid, that is, a mixing of epoxy and inorganic components on a nanoscale.

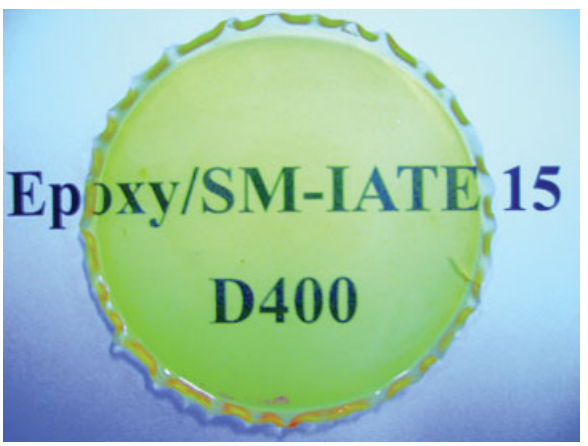

Figure 9 Photograph of the epoxy/SM-IATE 15 hybrid. [Color figure can be viewed in the online issue, which is available at www.interscience.wiley.com.]

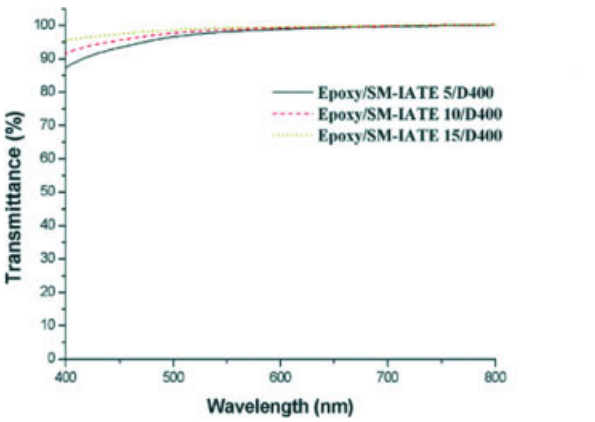

Figure 10 UV–vis spectra of the epoxy with different SM-IATE contents. [Color figure can be viewed in the online issue, which is available at www.interscience.wiley.com.]

UV–vis

Figure 10 shows the UV–vis spectra of the epoxy with different SM-IATE contents. There was no obvious absorbance over a range of 400–800 nm. This phenomenon revealed that the hybrids possessed excellent optical transparency. The transmit-

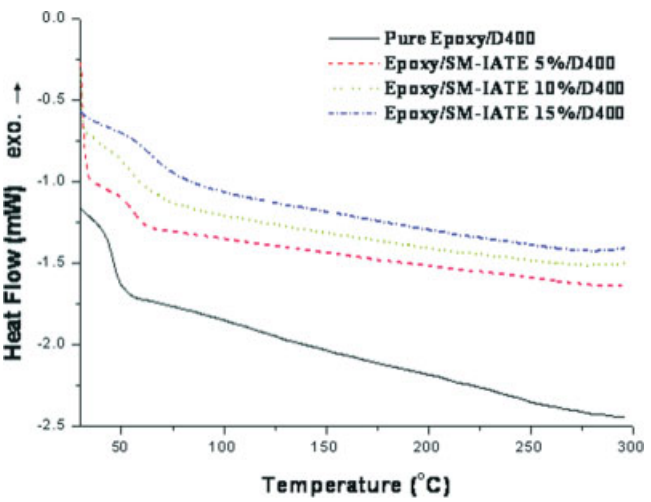

Figure 11 DSC of the epoxy resin with various SM-IATE contents. [Color figure can be viewed in the online issue, which is available at www.interscience.wiley.com.]

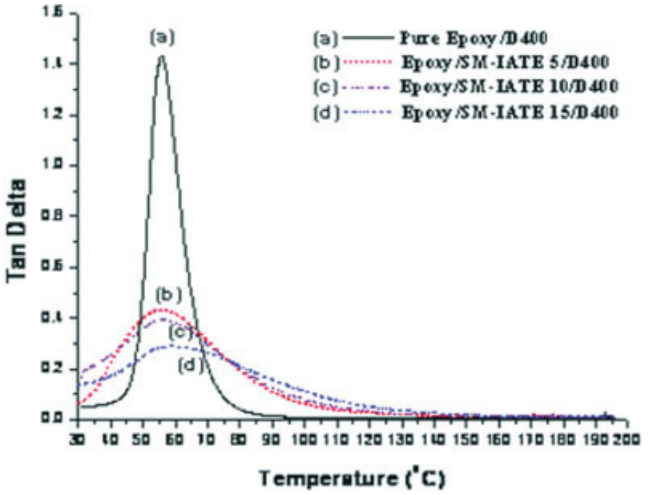

Figure 12 Temperature dependence of tan δ for the epoxy resin with various SM-IATE contents. [Color figure can be viewed in the online issue, which is available at www.interscience.wiley.com.]

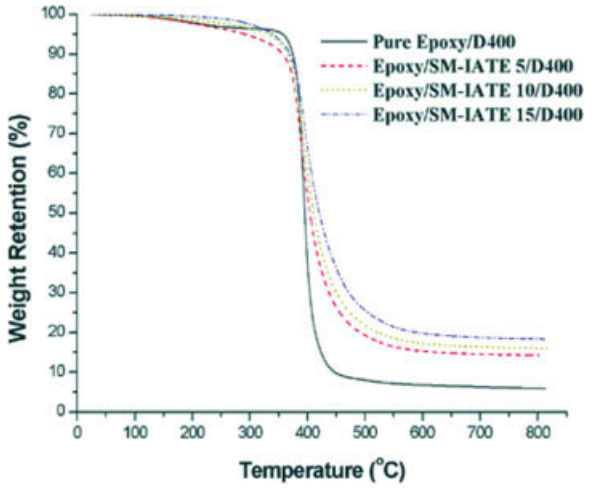

Figure 13 TGA thermograms of the epoxy resin with various SM-IATE contents. [Color figure can be viewed in the online issue, which is available at www.interscience.wiley.com.]

tance of the composites films increased slightly with an increasing amount of the inorganic moiety. This transmittance may be used as a criterion for the formation of a homogeneous phase. These results demonstrate the excellent optical transparency of the hybrids, which is the most important characteristic for their applications in protective coatings.

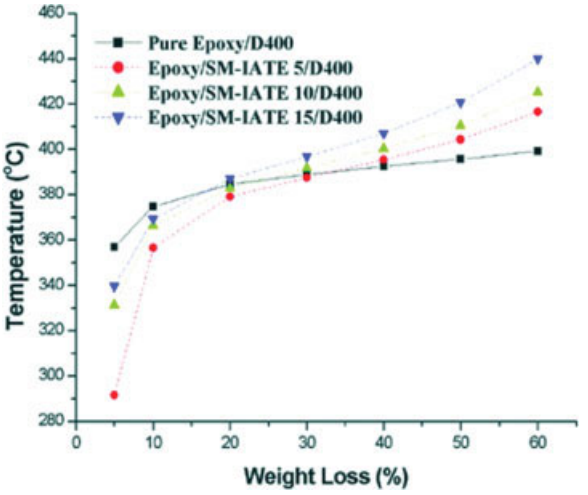

Figure 14 Weight-loss temperature versus the weight loss for the epoxy resin with various SM-IATE contents. [Color figure can be viewed in the online issue, which is available at www.interscience.wiley.com.]

Thermal properties

Figure 11 presents DSC curves of the epoxy resin with various SM-IATE contents. No obvious exothermic/endothermic peaks were observed, and this confirmed the high conversion of the condensation reaction of silanol groups in the curing reaction. The temperature at the baseline shift was read as T_g of the resin. T_g of the pure epoxy was 50°C. Introducing SM-IATE into the epoxy enhanced T_g of the resulting resins. The T_g values of the hybrids increased with increasing SM-IATE contents. Figure 12 shows the temperature dependence of tan δ (damping) for the epoxy resin with various SM-IATE contents. The tan δ peaks, which reflected the micro-Brownian segmental motions of the epoxy resin, were defined as T_g. The addition of the inorganic filler to the matrix made it difficult to move the polymer chain; therefore, the damping de-

TABLE II
Weight-Loss Characteristics of the Epoxy Resin with Various Amounts of SM-IATE

		Temperature at the characteristic weight loss (°C)							
	IPDT (°C)	5%	10%	20%	30%	40%	50%	60%	Residue at 800°C (%)
Pure epoxy	464	357	375	385	389	392	396	399	5.94
SM-IATE 5	594	292	357	379	388	395	404	417	14.23
SM-IATE 10	631	331	366	383	392	400	411	425	16.03
SM-IATE 15	689	340	369	387	397	407	421	440	18.37

The heating rate was equal to 10°C/min.

creased, and T_g was shifted to a higher temperature.[13] The relaxation strength (the height of the tan δ peak) decreased with increasing inorganic contents. Such a reduction of the tan δ peak for the organic–inorganic hybrid materials was attributed to the increase in the crosslinking of the polymer with the inorganic network or the entrapment of the polymer chains within the inorganic networks, resulting in the reduction of the polymer chain mobility.[14] The hybrids exhibited a single T_g; that is, they presented a homogeneous morphology. The tan δ peaks were broadened at higher inorganic contents, and this indicated an increase in the phase separation.[15,16]

TGA is one of the techniques commonly used for the rapid evaluation of the thermal stability of different materials, and it also indicates the decomposition of polymers at various temperatures. Figure 13 shows the TGA thermograms of the epoxy resin with various contents, from room temperature to 800°C, in a nitrogen atmosphere. Table II shows the weight-loss characteristics of the epoxy resin with various SM-IATE contents. Figure 14 shows the weight-loss temperature versus the weight loss for the epoxy resin with various SM-IATE contents. The thermal stability of the hybrids was lower than that of the pure epoxy when the thermal degradation just occurred. The Si—O group of SM-IATE was able to absorb more thermal energy, and its vibration could dissipate the thermal decomposition energy.[11] The char yields of the hybrids were higher than that of the pure epoxy at a high temperature. The high-temperature thermal stability could be increased with the addition of silicon-containing compounds because their products are silicon dioxide, which cannot be degraded further. The phenomenon revealed that the thermal stability of the hybrids increased with the contents of the inorganic components. Apparently, the enhancement of the thermal stability of the hybrids was achieved by the incorporation of silicon and nitrogen into the epoxy resins, which brought a Si—N synergistic effect.[17–19]

The integral procedure decomposition temperature (IPDT) proposed by Doyle[20] has been correlated to the volatile parts of polymeric materials and has been used for estimating the inherent thermal stability of polymeric materials.[21,22] According to Table II, the IPDT of the pure epoxy was 464°C, and the IPDTs of the hybrids were higher than that of the pure epoxy. The thermal stability of the hybrids increased with the contents of the inorganic components. The inorganic components could improve the thermal stability of the pure epoxy.

CONCLUSIONS

Novel epoxy nanocomposites containing silicon and nitrogen were prepared successfully via the sol–gel method. The structures of the monomers and composites were confirmed with FTIR, ^{1}H-NMR, and ^{29}Si-NMR. The results from SEM, EDX, and TEM revealed that the nanocomposites exhibited good compatibility between the organic and inorganic phases. The results of UV–vis and photographs demonstrated the excellent optical transparency of the hybrids. The inorganic components enhanced the thermal stability of the epoxy. Because of their optical transparency and high thermal stability, epoxy nanocomposites may have potential applications in protective coatings at elevated temperatures.

References

1. Gilman, J. W.; Jackson, C. L.; Morgan, A. B.; Harris, R.; Manias, E.; Giannelis, E. P.; Wuthenow, M.; Hilton, D.; Philips, S. H. Chem Mater 2000, 12, 1866.
2. Gilman, J. W. Appl Clay Sci 1999, 15, 31.
3. Morgan, A. B. Polym Adv Technol 2006, 17, 206.
4. Cho, J. D.; Ju, H. T.; Hong, J. W. J Polym Sci Part A: Polym Chem 2005, 43, 658.
5. Hajji, P.; Jonschker, G.; Goedicke, S.; Menning, M. J Sol–Gel Sci Technol 2000, 19, 39.
6. Ochi, M.; Takahashi, R.; Tenanchi, A. Polymer 2001, 42, 5151.
7. Tong, Y.; Liu, Y.; Ding, M. J Appl Polym Sci 2002, 83, 1810.
8. Walter, R. N.; Lyon, R. E. J Appl Polym Sci 2002, 87, 548.
9. Ray, S. S.; Okamoto, M. Prog Polym Sci 2003, 28, 1539.
10. Brinker, C. J.; Scherer, G. W. Sol–Gel Science: The Physics and Chemistry of Sol–Gel Processing; Academic: London, 1990.
11. Bandyopadhyay, A.; Bhowmick, A. R.; De Sarkar, M. J Appl Polym Sci 2004, 93, 2579.
12. Chiang, C. L.; Ma, C. C. Eur Polym J 2002, 38, 2219.
13. Cousin, P.; Smith, P. J Polym Sci Part B: Polym Phys 1994, 32, 459.
14. Tai, H.; Sargienko, A.; Silverstein, M. S. Polymer 2001, 42, 4473.
15. Zoppi, R. A.; Castro, C. R.; Yoshida, I. V. P.; Nunes, S. P. Polymer 1997, 38, 5705.
16. Tian, D.; Blacher, S.; Jerome, R. Polymer 1999, 40, 951.
17. Joseph, R.; Zhang, S.; Ford, W. Macromolecules 1996, 29, 1305.
18. Lu, S. Y.; Hamerton, I. Prog Polym Sci 2002, 27, 1661.
19. Liu, Y. L.; Chou, C. I. Polym Degrad Stab 2005, 90, 515.
20. Doyle, C. D. Anal Chem 1961, 33, 77.
21. Jelena, M.; Ivan, B.; Sebastijan, O.; Hrvoje, I.; Marica, I. Polym Degrad Stab 2006, 91, 122.
22. Park, S. J.; Kim, H. C.; Lee, H. I.; Suh, D. H. Macromolecules 2001, 34, 7573.